

## Indices of environmental variability in the Indian Ocean 1970-2005

Francis Marsac

IRD, UR 109 THETIS  
Centre de Recherche Halieutique  
BP 171, 34230 Sète cedex, France

### Introduction

The environmental variability of the Indian Ocean is described by time series of climatic and oceanographic variables for the period 1970-2005 in two areas located West and East of the ocean basin. Additional information on sea surface chlorophyll in the equatorial region illustrates the response of the base level of the pelagic ecosystem to the interannual climate forcing.

### Data and methods

Six environmental datasets were processed:

1. the monthly  $u$  (zonal) and  $v$  (meridian) components of the pseudo wind stress produced by the Florida State University (Tallahassee, FL)
2. the Extended Reconstructed Sea Surface Temperatures, version 2 (ERSST.v2) of the NCDC (Smith and Reynolds 2004);
3. the 2°latitude-by-5° longitude reanalysis of all quality controlled vertical temperature profiles (White 1995) available at the Joint Environmental Data Center (SIO, La Jolla, CA) from which the temperature at depth were interpolated to compute the depth of the 20°C isotherm (a proxy of the thermocline depth);
4. the Sea Surface Chlorophyll field by week and 9 km resolution, as measured by SeaWiFS for the period 1997-2002
5. the Topex sea surface height (SSH) anomalies, at a resolution of 10 days and 1° latitude-longitude boxes;
6. the sea level pressure (SLP) anomalies at two sites of the Indian Ocean, Mahe (Seychelles, West Indian Ocean) and Darwin (Australia).

For datasets (1) to (3), we extracted the data in two boxes (Fig. 1): West Indian Ocean, 50°E-70°E/5°N-10°S (Box 1) and East Indian Ocean, 90°E-110°E/0°-10°S (Box 2), computed anomalies from a monthly climatology 1970-90 and performed an EOF (Empirical Orthogonal Functions) analysis. The first mode of the EOFs was kept and the temporal structure is displayed as the times series relevant to each variables. The PC1 of the EOF analysis explains most of the variance as shown in Table 1.

The Sea Surface Chlorophyll (dataset 4) was extracted in the equatorial region (40°E-100°E / 2°N-10°S) (Fig. 1).

The Topex SSH anomalies (dataset 5) were extracted in two sub-areas T1 and T2 (Fig. 1).

Table 1 – Percentage of variance explained by the first EOF (PC 1) in the two boxes

Variable	Box 1	Box 2
Meridian wind stress	45.6 %	50%
Zonal wind stress	43 %	57.2 %
SST	84%	85%
Depth of mixed layer	40.2 %	64.2 %

The dataset (6) was used to compute a climatic index, the Indian Oscillation Index (Marsac & Le Blanc 1998) or IOI. Just like the SOI, this index is the difference of standardized SLP anomalies at two distant sites, namely Mahe and Darwin ( $IOI = SLP_{Astd} \text{ Seychelles} - SLP_{Astd} \text{ Darwin}$ ).

## Results

### 1- Long term trends

The zonal and meridional wind-stress components (Fig 2 a-d) point out a decade (1990 to 2002) of intense trade winds compared to the period prior to 1990. This fact is clearly denoted by concomitant intensification of both southerly and easterly flux. In the WIO, the transition is more rapid than in the EIO. The series of SSTA (Fig 2 e-f) displays dominant negative values until the end of the 80s, then positive anomalies up to present. The patterns depicted by these different variables are similar in the two area boxes under study.

The mixed layer (ML, Fig 2 g-h) becomes significantly deeper in the WIO from 1992, peaking in early 1998. Other (but transient) situations of deep thermocline were observed in 1972, 1978 and 1983. Except in 1988 and 2002, a good coherence is found in the WIO between a deep ML and the warm episodes traced by the SSTA. Conversely, this coherence is not found in the EIO, where the general pattern of the ML dynamics is even opposite to that observed in the WIO: deep thermocline occurred prior to 1987 (with negative SST anomalies) and shallow thermocline prevailed from 1987 to 1998.

### 2 – Interannual climate variability

It has been suggested that the Indian Ocean exhibits strong coupled ocean-atmosphere-land interactions that produce important perturbations to the annual cycle. Consequently, the Indian Ocean would not be a passive player to the ENSO/Southern Oscillation remote forcing originated in the Pacific (Webster et al 1999). Indeed, several warm episodes in the Indian Ocean have been recorded in the absence of any El Niño. A dipole structure characterizes the SST anomalies during the warm events (Saji et al 1999). In order to monitor the climatic variability in a way that is specific to the Indian Ocean, Marsac & le Blanc (1998) defined an atmospheric index, the Indian Oscillation Index (IOI). IOI and SST anomalies fluctuate in opposition. They are well correlated in the West Indian Ocean ( $r = -0.70$ ,  $p < 0.001$ ) as shown in Fig. 3. The correlation between the SOI and West Indian Ocean SST anomalies is -0.59. The correlation between the IOI and SST anomalies drops to -0.27 in the East Indian Ocean. Thus, the IOI can be considered as a good and simple descriptor of the hydroclimatic variability affecting the West Indian Ocean.

During warm events, the slope of the ocean reverses. The Eastern and Western Indian Ocean exhibit opposite patterns in the thermocline topography, as evidenced by time series of the Topex-Poseidon sea surface height anomalies in two sub-regions (T1 and T2) (Fig 4). The normal pattern is a rising slope from West to East, but during strong warm anomalies, the slope reverses and an upwelling is enhanced in the East, as a result of Ekman transport caused by strong alongshore winds off Sumatra.

### 3- Impact on the distribution of the purse seine catch

The full development of the 1997-98 warm anomaly occurred at the season when purse seiners are targeting large schools of yellowfin tuna congregating for spawning (Fig. 5a). The warm anomaly caused a dramatic drop in school occurrence and the deep thermocline (traced by positive sea surface height anomalies) reduced the vulnerability of fish to the purse seine. The fleet shifted eastward, following some type of gradient in school occurrence and catches. The best catches were made in the area influenced by the anomalous upwelling (traced by negative sea surface height anomalies), off Indonesia (Fig 5b). The following year, when conditions were back to normal, the highest catches were made in the traditional western fishing ground (Fig. 5c).

The longitude-time diagram of SeaWiFS sea colour anomalies (Fig.6) provides complementary insight related to biological production. The seasonal enrichment due to the Somalian upwelling appears in the middle of the year. A secondary enrichment occurs at the turn of the year along the African coast (42°E). During the peak of the 1997-98 warm event, an anomalous pattern of primary productivity is observed in the equatorial band. The enrichment at 42°E disappears and the overall productivity in the WIO is dramatically reduced. Conversely, the productivity becomes anomalously high in the East (85°E-100°E) in relation with the upwelling off Sumatra. The occurrence of tuna schools in the WIO drops at the end of 1997 and the catches are made downstream the area of enhanced primary production, during the 2 months following the peak chlorophyll anomaly. The time and space lag can reflect the development of a food chain up to prey consumed by tuna. During the following years (1998 to 2001), the positive chlorophyll anomalies in the Eastern basin tend to decrease. At the same timescale, the eastward boundary of the purse seine catches shifts back to the West. On the overall, the catches made at the turn of the year (yellowfin spawning season) are distributed at the edge of chlorophyll patches, suggesting a strong influence of forage availability on the concentration of spawners (and subsequently, larvae).

## References

Marsac F. & J-P. Hallier (1991). The recent drop in the yellowfin catches by the Western Indian Ocean purse seine fishery: overfishing or oceanographic changes? 4<sup>th</sup> Expert Consultation on Indian Ocean Tunas, Bangkok, Thailand, 2-6/07/90. *IPTP Coll. Vol. Work. Doc.*, 4: 66 – 83

Marsac F. & J-L Le Blanc J-L.(1998). Interannual and ENSO-associated variability of the coupled ocean-atmosphere system with possible impacts on the yellowfin tuna fisheries of the Indian and Atlantic oceans. *In* : J.S. Beckett (Ed). ICCAT Tuna Symposium. Coll. Vol. Sci. Pap., L(1) : 345-377

Webster P. et al. (1999). Coupled ocean-atmosphere dynamics in the Indian Ocean during 1997-98. *Nature* 401: 356-360

Saji N.H. et al. (1999). A dipole mode in the tropical Indian Ocean. *Nature* 401: 360-363

Smith T.M. and R.W. Reynolds (2004). [Improved Extended Reconstruction of SST \(1854-1997\)](#). *J. of Climate*, **17**, 2466-2477

White W.B. (1995). Design of a global observing system for gyre-scale upper ocean temperature variability. *Prog. Oceanogr.* 36 : 169-217

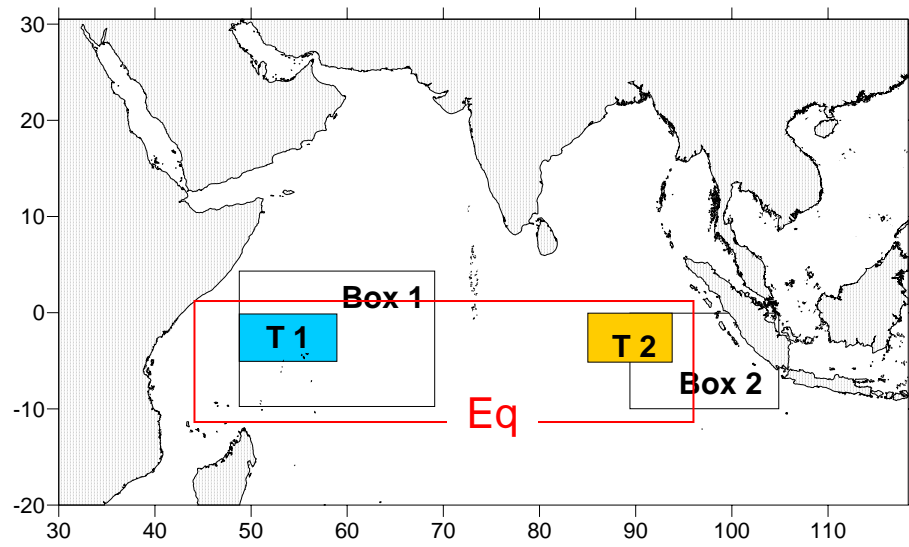


Fig 1 - Map of study areas. The boxes delineate the regions of the equatorial Indian Ocean where environmental series are reconstructed. The Topex sea surface height anomalies are studied in the two sub-areas T1 and T2. The Sea Surface Chlorophyll is extracted in the “Eq” box.

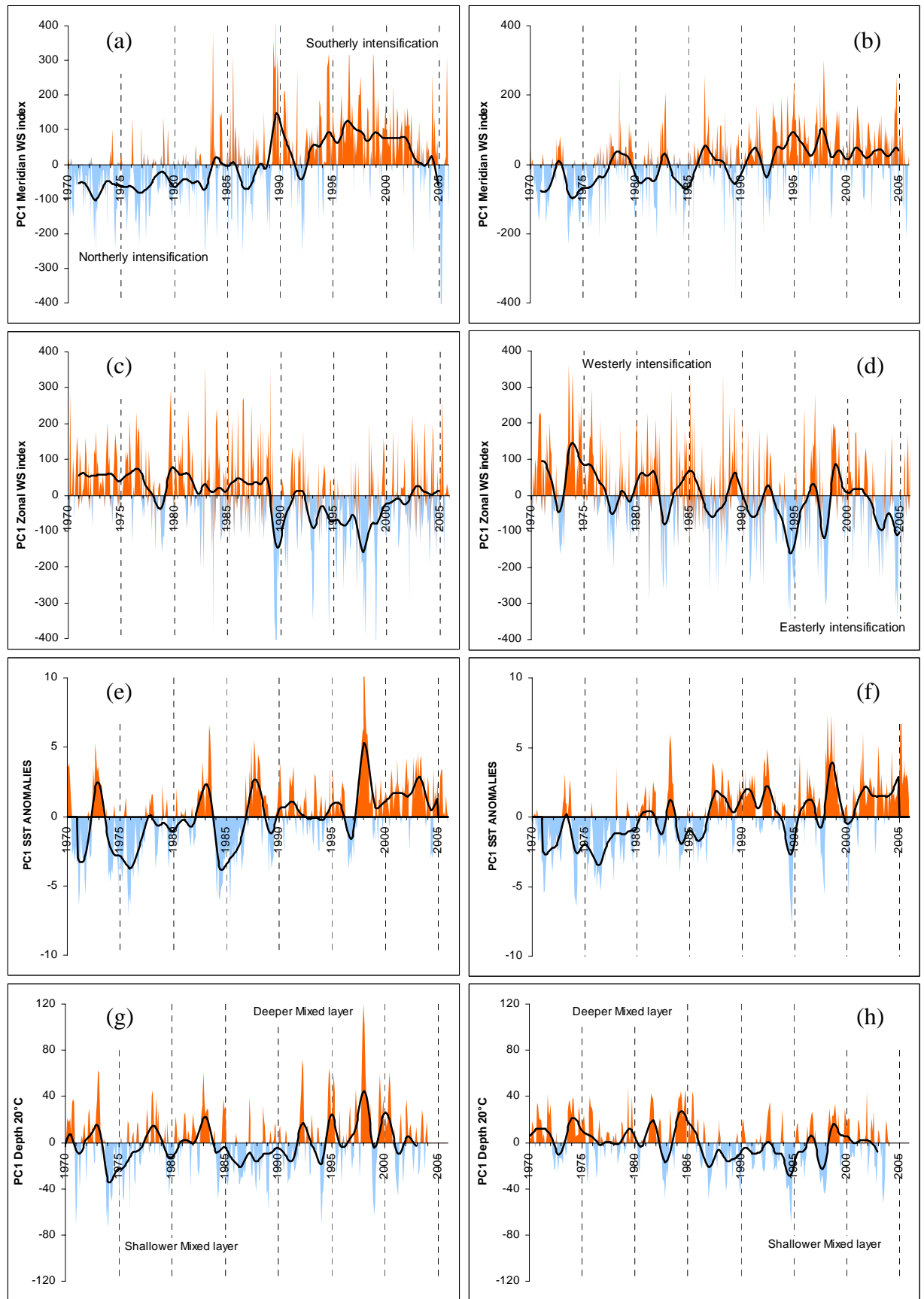


Fig 2 – Time series of the first mode of Empirical Orthogonal Functions (PC 1) for meridian (a-b) and zonal (c-d) components of wind stress, SST anomalies (e-f) and topography of the 20°C isotherm (g-h). Left column refers to Box 1 (WIO) and right column refers to Box 2 (EIO).

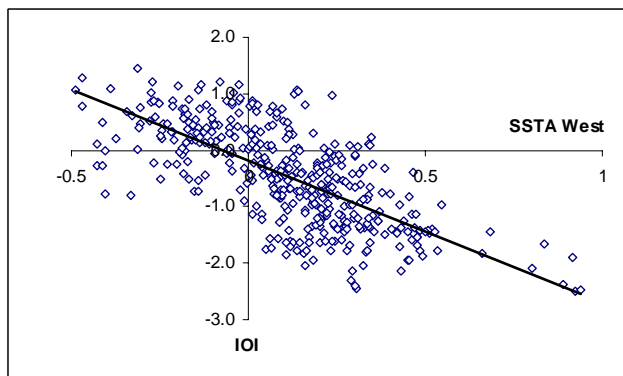
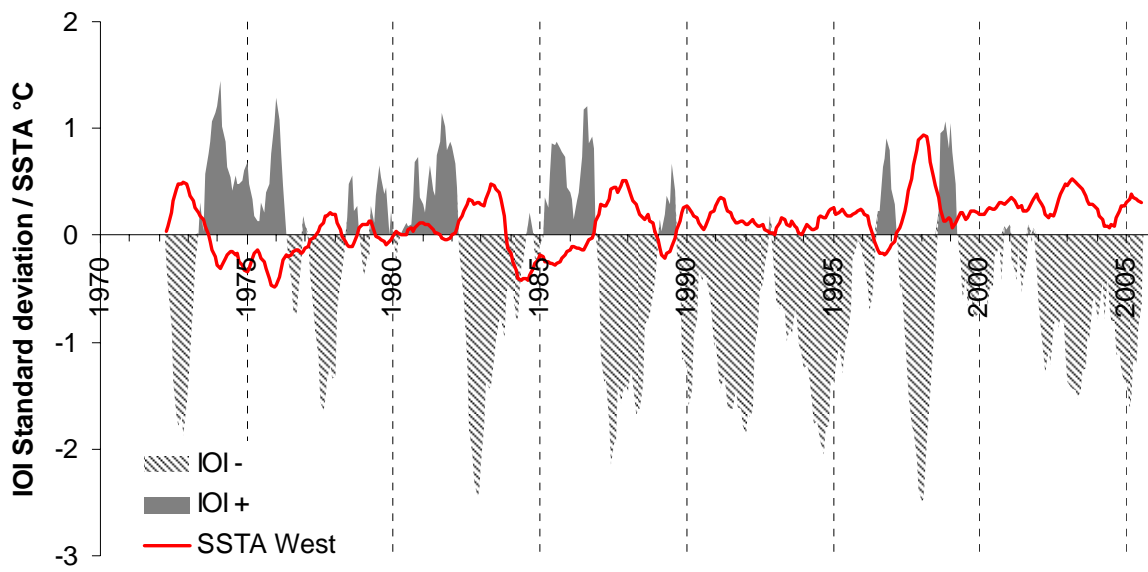


Fig 3 – Relationship between the Indian Oscillation Index (IOI) and the SST anomalies in the West Indian Ocean: (a) time series and (b) scatter plot ( $r = -0.70$ ,  $p < 0.001$ )

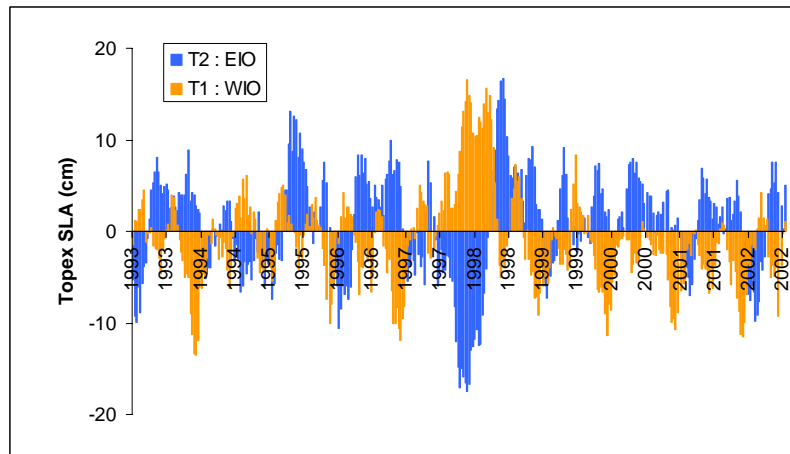


Fig 4 – Topex sea surface height anomalies in two sub areas (WIO and EIO). The dipole structure was particularly developed during the 1997-98 warm event.

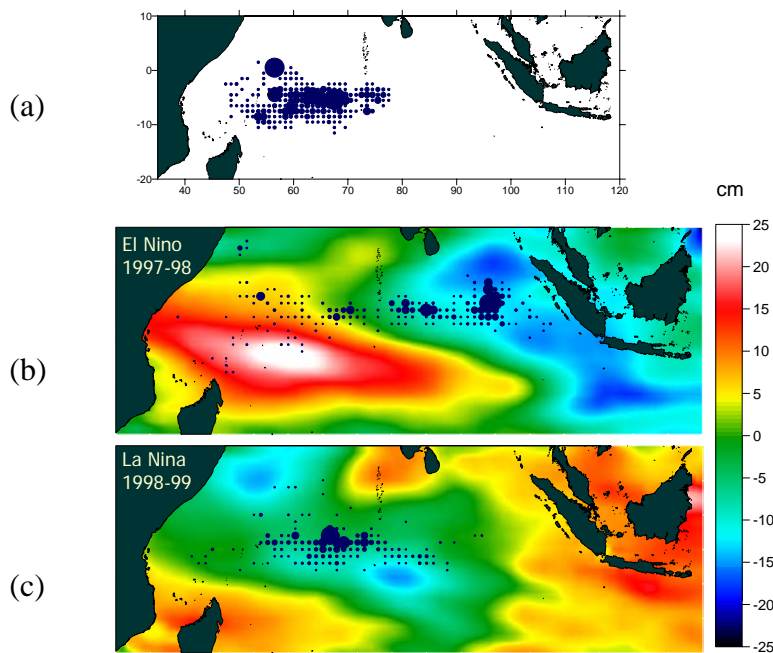


Fig 5 – Spatial shifts of the purse seine fishery during the 1997-98 ENSO in relation with sea level topography. Common distribution of the purse seine catches during the first quarter of the year (a); Topex sea surface height anomalies (color background) and purse seine catches in December 1997 (b) and in December 1998 (c). PS catches are represented by the black circles; the area of the circles is proportional to the catch.



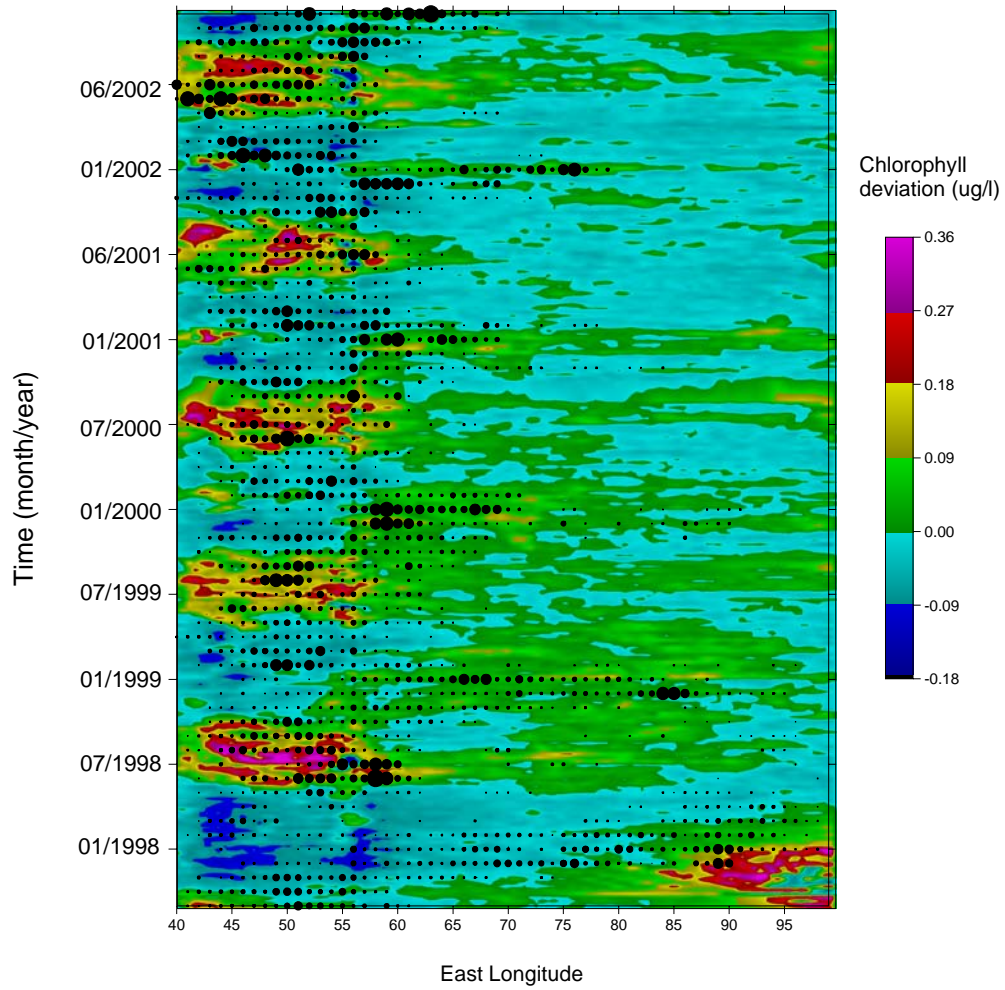


Fig 6 – Longitude-time diagram of SeaWiFS-derived chlorophyll content anomalies (colour background) and purse seine catches (black circles) from September 1997 to December 2002 at the equator ( $2^{\circ}\text{N}$ - $5^{\circ}\text{S}$ ). The catches (black circles) are summed over the  $2^{\circ}\text{N}$ - $5^{\circ}\text{S}$  equatorial band at each longitude step. Chlorophyll anomalies range from  $-0.18$  to  $+0.36 \mu\text{g.l}^{-1}$ . The anomalies at each time step (week) are the departures about the overall mean over the whole period (245 weeks).